

Color Image Watermarking Using Multidimensional Fourier Transforms

Tsz Kin Tsui, *Student Member, IEEE*, Xiao-Ping Zhang, *Senior Member, IEEE*, and Dimitrios Androutsos, *Senior Member, IEEE*

Abstract—This paper presents two vector watermarking schemes that are based on the use of complex and quaternion Fourier transforms and demonstrates, for the first time, how to embed watermarks into the frequency domain that is consistent with our human visual system. Watermark casting is performed by estimating the just-noticeable distortion of the images, to ensure watermark invisibility. The first method encodes the chromatic content of a color image into the CIE a^*b^* chromaticity coordinates while the achromatic content is encoded as CIE L tristimulus value. Color watermarks (yellow and blue) are embedded in the frequency domain of the chromatic channels by using the spatiochromatic discrete Fourier transform. It first encodes a^* and b^* as complex values, followed by a single discrete Fourier transform. The most interesting characteristic of the scheme is the possibility of performing watermarking in the frequency domain of chromatic components. The second method encodes the $L^*a^*b^*$ components of color images and watermarks are embedded as vectors in the frequency domain of the channels by using the quaternion Fourier transform. Robustness is achieved by embedding a watermark in the coefficient with positive frequency, which spreads it to all color components in the spatial domain and invisibility is satisfied by modifying the coefficient with negative frequency, such that the combined effects of the two are insensitive to human eyes. Experimental results demonstrate that the two proposed algorithms perform better than two existing algorithms—ac- and discrete cosine transform-based schemes.

Index Terms—Color, data hiding, digital image watermarking, quaternion Fourier transform (QFT), spatiochromatic discrete Fourier transform (SCDFT).

I. INTRODUCTION

THE success of the Internet and digital consumer devices has profoundly changed our society and daily lives by making the capture, transmission, and storage of digital data extremely easy and convenient. However, this raises a big concern in how to secure these data and preventing unauthorized use. This issue has become problematic in many areas. For example, there are many studies showing that the music and video industry loses billions of dollars per year due to

Manuscript received December 7, 2006; revised October 21, 2007. The associate editor coordinating the review of this manuscript and approving it for publication was Dr. Reginald Lagendijk.

T. K. Tsui is with Research In Motion, Waterloo, ON N2L 3W8, Canada (e-mail: tomtsui@gmail.com).

X.-P. Zhang and D. Androutsos are with the Department of Electrical and Computer Engineering, Ryerson University, Toronto, ON M5B 2K3, Canada (e-mail: xzhang@ee.ryerson.ca; dimitri@ee.ryerson.ca).

Color versions of one or more of the figures in this paper are available online at <http://ieeexplore.ieee.org>.

Digital Object Identifier 10.1109/TIFS.2007.916275

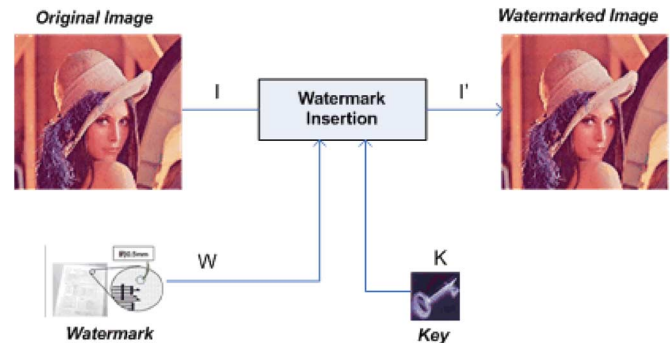


Fig. 1. Generic watermark insertion.

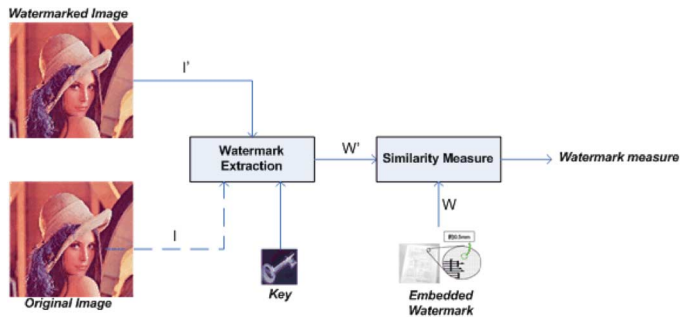


Fig. 2. Generic watermark extraction.

illegal copying and downloading of copyrighted materials from the Internet. Researchers have focused on methods and algorithms to address this issue—digital watermarking. The basic idea is to embed some secret data in digital content that is to be protected, and “seal” it within the content. Fig. 1 is a generic watermarking insertion process. Original digital media is inserted into a watermarking system by using a key. The system produces a watermarked work. Fig. 2 shows a generic watermarking extraction process.

Digital images, in particular, are one type of digital media that warrants extra attention when it comes to digital watermarking. A digital image is composed of a set of pixels, which can be conveniently captured by many electronic devices, such as digital cameras, scanners, and camcorders. Each pixel of an image is usually associated with a spatial coordinate in some 2-D region, which has a value consisting of one or more samples. Due to the ease of network connectivity and the proliferation of digital image capture devices, the access and sharing of images has become extremely feasible and convenient. However, some access and sharing may be unauthorized or illegal. Thus, digital image watermarking has become an active research area focused on

battling these types of activities. In general, digital image watermarking schemes mainly fall into two broad categories—spatial-domain and transform-domain techniques.

A. Spatial-Domain Techniques

Least-Significant Bit (LSB): The earliest work of digital image watermarking schemes can be traced back to the early 1990s [1], where the idea was to embed watermarks in the LSB of the pixels. Given an image with $N \times N$ pixels, and each pixel being represented by an 8-b sequence (s_1, s_2, \dots, s_8) , the watermarks are embedded in the last (i.e., least significant), bit, s_8 of selected pixels of the image. This method is easy to implement and does not generate serious distortion to the image; however, it is not very robust against attacks. For instance, an attacker could simply randomize all LSBs, which effectively destroys the hidden information.

Patchwork [2]–[4]: The objective of this method is to answer the question: Does this image contain a watermark? The process begins by pseudorandomly choosing n -ordered pairs (a_i, b_i) of pixels of the image, followed by the operation:

$$(a_i, b_i) \longleftrightarrow (a_i + 1, b_i - 1). \quad (1)$$

The extraction process for the patchwork watermark proceeds by choosing the same n -ordered pairs of pixels. The receiver then sums the value $(a_i - b_i)$ for all n values of i . The watermark is detected if this sum is around $2n$ and is not detected otherwise.

SSM-modulation-based techniques [5], [6]: Spread-spectrum techniques are methods in which energy generated at one or more discrete frequencies is deliberately spread or distributed in time or frequency domains. This is done for a variety of reasons, including the establishment of secure communications, increasing resistance to natural interference and jamming, and to prevent detection. When applied to the context of image watermarking, SSM-based watermarking algorithms embed information by linearly combining the host image with a small pseudonoise signal that is modulated by the embedded watermark.

B. Transform-Domain Techniques

Compared to spatial-domain methods, frequency-domain methods are more widely applied. The aim is to embed the watermarks in the spectral coefficients of the image. The most commonly used transforms are the discrete cosine transform (DCT), discrete Fourier transform (DFT), discrete wavelet transform (DWT), discrete Laguerre transform (DLT) and the discrete Hadamard transform (DHT). The reasons for watermarking in the frequency domain is that the characteristics of the human visual system (HVS) are better captured by the spectral coefficients. For example, the HVS is more sensitive to low-frequency coefficients, and less sensitive to high-frequency coefficients [7]. In other words, low-frequency coefficients are perceptually significant, which means alterations to those components might cause severe distortion to the original image. On the other hand, high-frequency coefficients are considered insignificant; thus, processing techniques, such as compression, tend to remove high-frequency coefficients aggressively. To

obtain a balance between imperceptibility and robustness, most algorithms embed watermarks in the midrange frequencies.

DCT-Based Approach: Cox [8] first proposed an algorithm that inserts watermarks into the spectral components of the image using techniques analogous to spread-spectrum communication [9]. The algorithm is to place the watermark into a set of frequency components that are perceptually significant. It has been shown that the watermarks are very hard to detect because they consist of relatively weak noise signals. In addition, placing the watermarks in the frequency domain would spread them over all pixels, which increases the robustness, and reliability against an unintentional or intentional attack.

Similar algorithms to watermark in the DCT domain were proposed in [10] and [11]. They incorporate a just noticeable difference (JND) profile [12] to determine the maximum amount of the watermark signal that can be tolerated at each region in the image without degrading its visual quality. The estimation of the JND is usually based on the properties of the HVS, such as spatial masking and luminance contrast [13].

DWT-Based Approach: Wang and Pearmain [14] proposed a wavelet-based watermarking algorithm based on the principle of multithreshold wavelet codec (MTWC). It searches the significant wavelet coefficients to embed the watermarks in order to increase robustness. Podilchuck and Zeng [15] proposed an adaptive watermarking algorithm according to the JND threshold. Kaewkamnerd [16] proposed a wavelet-based scheme that employs the characteristics of the HVS to determine the weighting function to adjust the watermark strength.

DLT-Based Approach: In 2000, Piva *et al.* [17] proposed a watermarking scheme using the DLT and DFT together. The DLT is first applied to the RGB components of the image, then watermarking is performed independently in the DFT domain of the Karhunen–Loeve (KL)-transformed bands. Watermark embedding is achieved by modifying the magnitude of midfrequency DFT coefficients. A Bayesian decision is used to optimally detect the presence of the watermark by the detector. In the same year, Gilani [18] also conducted extensive performance comparisons between DLT- and DCT-domain watermarking schemes. He concluded that the quality of the DLT-domain watermarked images is higher than the corresponding DCT-domain watermarked images, while maintaining the same robustness.

DHT-Based Approach: Ho [19] and Gilani [20] proposed an algorithm in 2002 that uses the DHT for data embedding. The advantage is that it offers much shorter processing time and easier hardware implementation. Thus, it is optimal for real-time applications.

DFT-Based Approach: Fourier coefficients have two components—phase and magnitude. Experiments have shown that attacks, such as geometric rotation, do not modify the phase information of the coefficients. Therefore, many DFT-based algorithms have been proposed that are robust to translation, rotation, and scaling attacks. Licks' algorithm [21] is one example.

Others: Most of the existing watermarking schemes mentioned before were designed to mark greyscale images, which ignore the correlation between different color channels. To overcome this problem, researchers have started to propose models to process the color channels intrinsically. For example, Reed

and Hannigan proposed a system that takes advantage of the low sensitivity of the HVS to high-frequency changes along the yellow–blue axis, to place most of the watermark in the yellow component of the image [22]. Bas *et al.* proposed a digital color image watermarking scheme using the hypercomplex numbers representation and the quaternion Fourier transform (QFT) [23].

II. BACKGROUND AND MOTIVATION

One of the main challenges of the watermarking problem is to achieve a better tradeoff between robustness and perceptivity. From an engineering perspective, these are two conflicting requirements that cannot be satisfied at the same time. Robustness can be achieved by increasing the strength of the embedded watermark, but the visible distortion would be increased as well. To deal with this problem effectively, the characteristics of the HVS have to be considered thoroughly in order to increase the perceptivity. Even though many HVS-based watermarking schemes have been invented, only a small portion of them were specifically designed for color images. This is due to a number of reasons: First, an objective and perceptual metric for color distortion is lacking; as a result, it is very hard to quantify how similar two images are. Second, we do not have a holistic transform that can process the color information of an image in a vector manner. This paper aims to exploit the chromatic information of color images, find appropriate transforms to bring the information to the frequency domain, and be able to embed watermarks as vectors into the chromatic as well as the luminance channels. This paper uses the theory of spatiochromatic image processing (SCIP), proposed by McCabe in 2000 [24] to develop two new color watermarking schemes.

Spatiochromatic image processing encodes only the color information of an image (for example, a^* and b^* channels in the $L^*a^*b^*$ color space) to complex numbers $a + jb$, and analyze it via one complex frequency transform—the spatiochromatic discrete Fourier transform (SCDFT) [24], which is defined as follows:

$$A(P, Q) + jB(P, Q) = \sum_{p=-\frac{N}{2}+1}^{\frac{N}{2}} \sum_{q=-\frac{N}{2}+1}^{\frac{N}{2}} [a^*(p, q) + jb^*(p, q)] \times e^{\frac{(-2\pi j(Pp+Qq))}{N}} \quad (2)$$

and the inverse SCDFT is defined as

$$a^*(p, q) + jb^*(p, q) = \sum_{P=-\frac{N}{2}+1}^{\frac{N}{2}} \sum_{Q=-\frac{N}{2}+1}^{\frac{N}{2}} [A(p, q) + jB(p, q)] \times e^{\frac{(2\pi j(Pp+Qq))}{N}} \quad (3)$$

where $N \times N$ is the size of the image, (p, q) are the image spatial coordinates, (P, Q) are the frequency coordinates, and (A, B) are the real and imaginary values occurring at the spatial frequency (P, Q) , which determines how the colors in the image change spatially.

Using the concept of phasors, the SCDFT coefficients can be interpreted as rainbow gratings rotating along the circular path

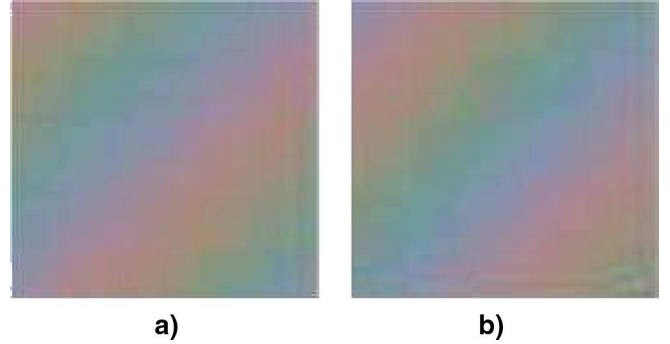


Fig. 3. Spatiochromatic frequency gratings defined at 1 cycle/image in the x and y directions and circular color modulation paths in color space. (a) Initial phases = 0. (b) Initial phase = $-(\pi/2)$.

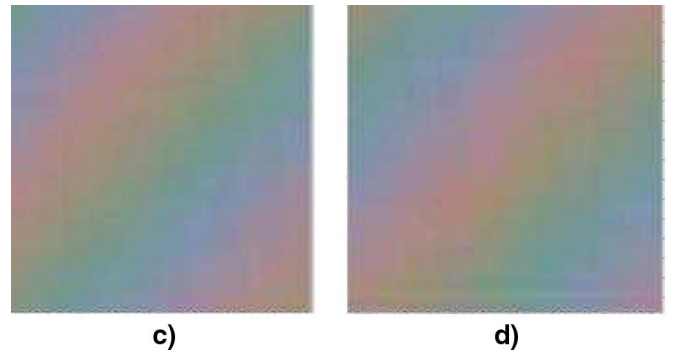


Fig. 4. (a) Initial phases = $-\pi$. (b) Initial phase = $\pi/2$.

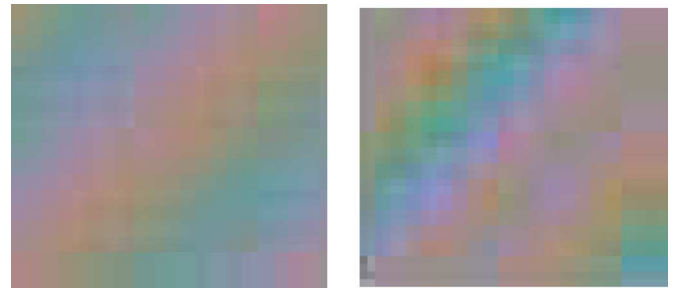


Fig. 5. (a) Color pattern with 1 revolution/cycle. (b) Color pattern with 2 revolutions/cycle.

containing the a^* and b^* components. One important observation is that the magnitude of the SCDFT coefficient $A(P, Q) + jB(P, Q)$ can be used to represent the saturation of the color, and the phase (angle) can represent its hue. Figs. 3 and 4 show examples of basis functions produced when either the negative- or the positive-frequency component is zero, generating an oscillation through all colors. The rainbow gratings in the figures oscillate in the same direction, but different phases. The initial phases are 0, $-(\pi/2)$, $-\pi$, and $\pi/2$, respectively. In addition, one color pattern can have different oscillation frequencies, which is shown in Fig. 5.

One interesting thing about McCabe's theory is that it allows us to generate spatial frequencies with modulations operating in either the red–green or the yellow–blue color opponency paths, if $A(P, Q)$, $B(P, Q)$, $A(-P, -Q)$, $B(-P, -Q)$ satisfy the following conditions.

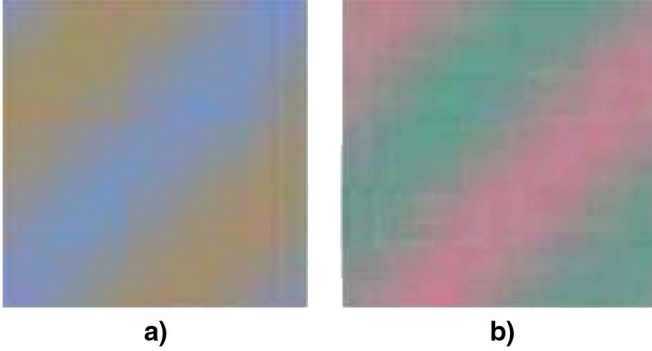


Fig. 6. Two different color patterns. (a) Yellow–blue pattern. (b) Red–green pattern.

- For variation along red–green, $A(P, Q) = k$, $B(P, Q) = 0$, $A(-P, -Q) = k$, and $B(-P, -Q) = 0$, such that the resulting path only varies along the real axis.
- For variation along yellow–blue, $A(P, Q) = 0$, $B(P, Q) = k$, $A(-P, -Q) = 0$, and $B(-P, -Q) = k$, which makes the resulting path vary along the imaginary axis.

Fig. 6 demonstrates the patterns for the aforementioned two conditions. The theory of color opponency paths is useful for the reason that by modifying the SCDFT coefficients in certain ways, a watermark with yellow–blue variation can be generated. Since the HVS is not sensitive to these colors, the imperceptibility of the watermark can be improved.

Color is, undoubtedly, an important feature in color images. Most digital images have three components, such as the red, green, and blue components in the RGB color space or the luminance (Y) and chrominance (u, v) components in the Yuv domain. The luminance/chrominance models, such as the Yuv , or the $La*b*$, are more frequently used in digital image processing, because they model human perception of color more closely than the RGB model. However, most existing watermarking algorithms do not take color information into account. These algorithms simply mark the luminance component only, while ignoring the chrominance. The motivation behind the work presented in this paper was to take advantage of the color content of digital images and to try and answer the question of how we can take advantage of the color contents in order to increase the robustness, or decrease the visible distortion. The proposed idea was inspired by the fact that colors can be added or subtracted to produce other colors. One characteristic of the HVS is that it is more sensitive to certain colors, such as red, and less sensitive to colors, such as blue [7]. If the watermark is embedded in the less sensitive area, then the strength of it can be increased and still be undetected by human eyes. However, this creates a problem. Many compression techniques, such as JPEG, eliminate the insensitive chromatic components aggressively, which might easily destroy the embedded watermark. On the other hand, if the watermark is embedded in the highly sensitive area, then the strength of it must be low in order to be invisible. The ultimate goal is to try and achieve both. However, these two criteria are conflicting requirements. So the question that arises is: How can a better tradeoff be achieved?

Intuitively, if a watermark is embedded in the low-frequency SCDFT coefficient $F(u, v)$, using the theory on SCIP, the effect is the same as adding a rainbow grating to the image. Since the watermark pattern is a rainbow grating that contains sensitive colors such as red and green, the watermark after embedding would be easily detected by the HVS. In order to decrease the visible distortion, our proposed algorithm adds one more step: to add a compensation pattern in the negative frequency $F(-u, -v)$.

This new approach would produce much lower visible distortion, due to the fact that only insensitive colors (e.g., yellow and blue) are added to the original image. Notice that the watermark still resides in the low-frequency coefficient. The purpose of adding the compensation mark in the negative coefficient is merely to decrease (i.e., compensate) the visible distortion generated by adding the watermark in the positive frequency coefficient.

From the decoder’s perspective, both approaches are exactly the same. The decoder would only look at the positive coefficient for watermark extraction, ignoring the compensation mark. In fact, the compensation mark would be most likely destroyed by external attacks. In other words, with everything remaining the same, the proposed approach generates lower distortion under the same watermark strength (i.e., higher imperceptibility with the same robustness). Having introduced the inspiration and logic, the technical details will now be given, including the discussion relevant for designing a comprehensive watermarking scheme, including the characteristics of the HVS, color spaces, and methodologies.

A. Human Visual System (HVS)

The HVS has been mentioned many times in the previous sections, but a clear description of it has not been given. In fact, this topic has been researched for many years [25], [26] and a single mathematical model that incorporates all masking effects is still unavailable. Nevertheless, a simpler model that considers some common masking effects related to image processing has been proposed. Specifically, the masking effects that are considered are luminance masking [25], [26]; texture masking [25], [27]; and frequency masking [28], [29].

Due to these visual inconsistencies in sensitivity of the HVS, there are perceptual redundancies inherited in an image. A quantity, called the JND [12] indicates the limit of the amount of information that can be added or subtracted from the image without sacrificing its visual quality. It is ideal for watermarking, because it gives an upper bound to the strength of the embedded watermark, such that the watermarked image would look the same as the original. To satisfy the invisibility requirement, the new algorithms proposed in this paper use the following characteristics to measure watermark robustness:

- the HVS is particularly sensitive to changes in image hue;
- the eye is less sensitive to the yellow–blue component [7];
- the JND model proposed by Chou in 2003 [30].

B. Color Spaces

A color model is an abstract mathematical model describing the way colors can be represented as tuples of numbers, typically as three or four values or color components. In the context

of watermarking, an objective metric to measure the perceptual distortion between the original image and watermarked image is definitely required. In this paper, the $L^*a^*b^*$ was chosen for the proposed algorithms because it is a uniform color space.

CIE $L^*a^*b^*$ (CIELAB) is the most complete color model conventionally used to describe all of the colors that are visible to the human eye [31]. It was developed for this specific purpose by the International Commission on Illumination (Commission Internationale d'Eclairage, hence its CIE initialism). The parameter L represents the lightness of the color (ranges from 0 to 100), whereas a^* and b^* are chromatic information.

The color difference ΔE at each pixel, is defined as

$$\Delta E = \sqrt{\Delta L^2 + (\Delta a^*)^2 + (\Delta b^*)^2}. \quad (4)$$

Experiments have shown that $\Delta E < 1$ is not detectable by the HVS, and $\Delta E < 3$ is not apparent [30]. $\Delta E = 3$ is called the uniform just-noticeable color difference (UJNCD), and Chou [30] derived a JND model, which he called the nonuniform just-noticeable color difference (NUJNCD) after considering some masking effects. His model produces a value $JND(L, a^*, b^*)$ for every pixel of a color image in the $L^*a^*b^*$ color space. As long as the distortion is less than this value, human eyes would not be able to detect the difference. This paper uses his model to bound the distortion generated by embedding the watermark. The next two sections introduce the algorithms using two multidimensional transforms—SCDFT and QFT.

III. NEW COLOR IMAGE WATERMARKING ALGORITHMS USING MULTIDIMENSIONAL FOURIER TRANSFORMS

A. SCDFT Image Watermarking [32]

Given an image of size $N \times N$, the image is divided into blocks of size 8×8 , followed by taking the SCDFT of each block. A pair of marks $w(k_1, k_2)$ and $w(-k_1, -k_2)$ are embedded into the coefficients $f(k_1, k_2)$ and $f(-k_1, -k_2)$ in the following way:

$$f'(k_1, k_2) = f(k_1, k_2) \pm \alpha w(k_1, k_2), \quad (5)$$

$$f'(-k_1, -k_2) = f(-k_1, -k_2) \pm \alpha w(-k_1, -k_2) \quad (6)$$

where α is the watermark strength to be maximized. To apply the two characteristics of the HVS as mentioned in Section III-A, some constraints are imposed to the values $w(k_1, k_2)$ and $w(-k_1, -k_2)$. Let

$$f(k_1, k_2) = f_{rp} + j f_{ip}, \quad (7)$$

$$w(k_1, k_2) = w_{rp} + j w_{ip}, \quad (8)$$

$$w(-k_1, -k_2) = w_{rn} + j w_{in} \quad (9)$$

where the subscript $r \equiv real$, $i \equiv imaginary$, $p \equiv positive$, $n \equiv negative$. From Section III-A, the HVS is particularly sensitive to changes in image hue, and less sensitive to the yellow–blue component. Therefore, the watermark should be designed to satisfy the following conditions:

1) *Keep the Hue (Angle) Unchanged*: Similar to most watermarking schemes, the watermark $w(k_1, k_2)$ is adjusted by a

scaling factor α , before being added to the coefficient $f(k_1, k_2)$. The equation is formulated as

$$f'(k_1, k_2) = f_{rp} + j f_{ip} \pm \alpha(w_{rp} + j w_{ip}) \quad (10)$$

where $f'(k_1, k_2)$ is the new coefficient. In general, $f(k_1, k_2)$ is a complex quantity that can be represented by its magnitude and angle. As described in the SCIP, the angle of an SCDFT coefficient is interpreted as the hue of a color corresponding to the chromaticity diagram. Our goal is to make the angle of $f'(k_1, k_2)$ to be the same as $f(k_1, k_2)$, which is $\tan^{-1}(f_{ip} \pm \alpha w_{ip} / f_{rp} \pm \alpha w_{rp}) = \tan^{-1}(f_{ip} / f_{rp})$. To achieve this requirement, we let $w_{rp} = p \times f_{rp}$ and $w_{ip} = p \times f_{ip}$, where p is a constant, which gives us

$$\begin{aligned} \tan^{-1} \left(\frac{f_{ip} \pm \alpha w_{ip}}{f_{rp} \pm \alpha w_{rp}} \right) &= \tan^{-1} \left(\frac{f_{ip}(1 \pm \alpha p)}{f_{rp}(1 \pm \alpha p)} \right) \\ &= \tan^{-1} \left(\frac{f_{ip}}{f_{rp}} \right). \end{aligned} \quad (11)$$

Thus, the requirement to keep the hue unchanged is fulfilled if $p = 1$, and so we get

$$w_{rp} = f_{rp}, w_{ip} = f_{ip}. \quad (12)$$

2) *Make the Overall Effect be Yellow–Blue*: According to McCabe's theory, if the summation of the real parts of the positive and negative frequency coefficients is zero, then the resulting path would vary along the yellow–blue axis of the chromaticity diagram. We can satisfy this condition by setting

$$w_{rn} = -w_{rp}, w_{in} = w_{ip} \quad (13)$$

since $w_{rn} = -w_{rp}$ cancels out the real part of the watermarks, only the imaginary part remains. Substituting (13) and (12) into (5) and (6) gives the result

$$f'(k_1, k_2) = f(k_1, k_2) \pm \alpha(f_{rp} + j f_{ip}), \quad (14)$$

$$f'(-k_1, -k_2) = f(-k_1, -k_2) \pm \alpha(-f_{rp} + j f_{ip}). \quad (15)$$

To ensure invisibility of the watermarks, a distortion metric $D(n, m, k_1, k_2)$ is defined to measure the difference in the spatial domain generated by modifying the coefficients $f(k_1, k_2)$ and $f(-k_1, -k_2)$ in the frequency domain formulated as

$$\begin{aligned} D(n, m, k_1, k_2) &= \frac{1}{N^2} \left((f(k_1, k_2) - f'(k_1, k_2)) e^{\left(\frac{2\pi j k_1 n}{N}\right)} e^{\left(\frac{2\pi j k_2 m}{N}\right)} \right. \\ &\quad \left. + (f(-k_1, -k_2) - f'(-k_1, -k_2)) \right. \\ &\quad \left. \times e^{\left(\frac{-2\pi j k_1 n}{N}\right)} e^{\left(\frac{-2\pi j k_2 m}{N}\right)} \right). \end{aligned} \quad (16)$$

Substituting (14) and (15) into (16) gives

$$\begin{aligned} D(n, m, k_1, k_2) &= \frac{1}{N^2} \left(-\alpha(f_{rp} + j f_{ip}) e^{\left(\frac{2\pi j k_1 n}{N}\right)} e^{\left(\frac{2\pi j k_2 m}{N}\right)} \right. \\ &\quad \left. -\alpha(-f_{rp} + j f_{ip}) e^{\left(\frac{-2\pi j k_1 n}{N}\right)} e^{\left(\frac{-2\pi j k_2 m}{N}\right)} \right). \end{aligned} \quad (17)$$

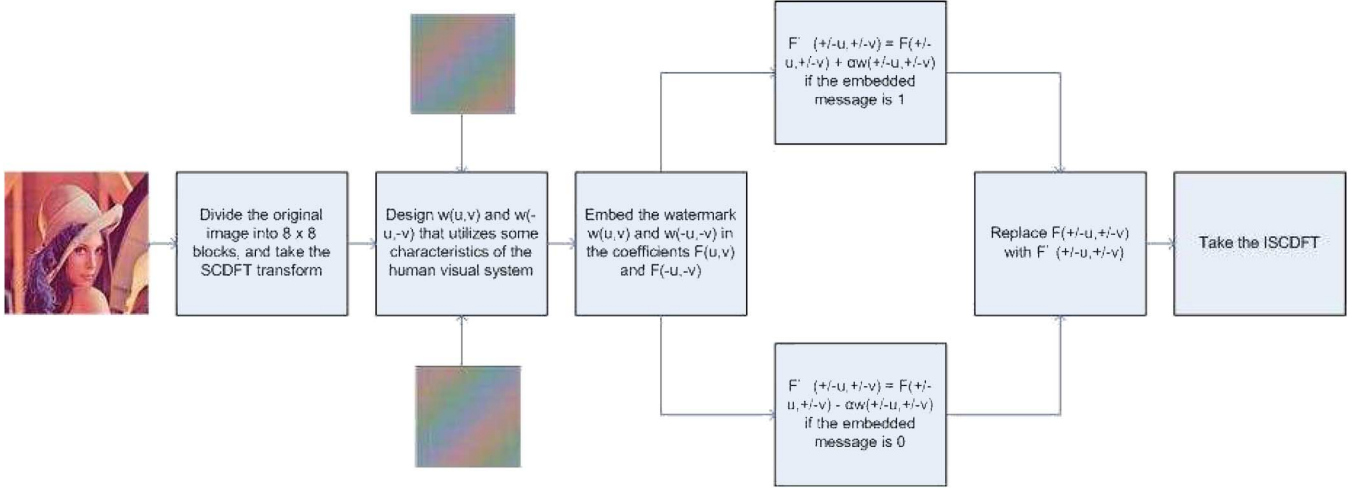


Fig. 7. Flow diagram showing the insertion procedure using the SCDFT scheme.

Let $\theta_1 = 2\pi k_1 n/N$ and $\theta_2 = 2\pi k_2 m/N$, noting that $e^x = \cos x + j \sin x$ and with some algebraic manipulations, (17) can be simplified to

$$D(n, m, k_1, k_2) = \frac{1}{N^2} (-j\alpha (2f_{rp}(\sin \theta_2 \cos \theta_1 + \sin \theta_1 \cos \theta_2) + 2f_{ip}(\cos \theta_1 \cos \theta_2 - \sin \theta_1 \sin \theta_2))). \quad (18)$$

To maximize the scaling factor α , we set the parameter NUJNCD to an upper bound of $D(n, m, k_1, k_2)$, that is, $D(n, m, k_1, k_2) < \text{NUJNCD}$ for every spatial coordinate n and m . Taking the square of both sides gives

$$\begin{aligned} \|D(n, m, k_1, k_2)\|^2 &= \frac{\alpha^2}{N^4} (2f_{rp}(\sin \theta_2 \cos \theta_1 + \sin \theta_1 \cos \theta_2) \\ &\quad + 2f_{ip}(\cos \theta_1 \cos \theta_2 - \sin \theta_1 \sin \theta_2))^2 \\ &\leq (\text{NUJNCD})^2. \end{aligned} \quad (19)$$

Depending on the perceptual requirement of the applications, two methods are available to determine α .

- Make the average distortions of a block less than NUJNCD (loose condition).
- Make the distortion of every pixel less than NUJNCD (tight condition).

Approach 1: Calculate α such that the average distortions of a block are less than NUJNCD

$$\begin{aligned} \|D(k_1, k_2)\|^2 &= \alpha^2 \sum_{n=0}^{N-1} \sum_{m=0}^{N-1} \frac{1}{N^4} (2f_{rp}(\sin \theta_2 \cos \theta_1 + \sin \theta_1 \cos \theta_2) \\ &\quad + 2f_{ip}(\cos \theta_1 \cos \theta_2 - \sin \theta_1 \sin \theta_2))^2 \\ &= N^2 (\text{NUJNCD})^2. \end{aligned} \quad (20)$$

Let $x = \cos \theta_1 \cos \theta_2 - \sin \theta_1 \sin \theta_2$ and $y = \sin \theta_2 \cos \theta_1 + \sin \theta_1 \cos \theta_2$

$$\alpha = \sqrt{\frac{N^6 (\text{NUJNCD})^2}{\sum_{n=0}^{N-1} \sum_{m=0}^{N-1} (2f_{rp}y + 2f_{ip}x)^2}}. \quad (21)$$

Approach 2: Recursively decrease α until the distortions of all pixels are smaller than NUJNCD. An initial α is assigned, and then $\|D(n, m, k_1, k_2)\|^2$ is calculated for every pixel of the block. If the distortion of some pixels exceeds $(\text{NUJNCD})^2$, α is decreased until $\|D(n, m, k_1, k_2)\|^2 < (\text{NUJNCD})^2 \forall n, m$.

In general, Approach 1 should be used when the robustness of the watermarks is critical while the invisibility constraint can be relaxed. On the other hand, Approach 2 is good for cases where the invisibility constraint is more important. The flow diagram showing the insertion procedure is illustrated in Fig. 7.

To extract the embedded watermarks, the original image and the watermarked (possibly corrupted) image are needed. $f(k_1, k_2) + \alpha(f_{rp} + jf_{ip})$ and $f(k_1, k_2) - \alpha(f_{rp} + jf_{ip})$ are calculated from the original image, followed by a distance comparison to the coefficient extracted from the watermarked image. If the extracted coefficient is closer to $f(k_1, k_2) + \alpha(f_{rp} + jf_{ip})$, we assume bit 1 was embedded; otherwise, bit 0 was embedded. The flow diagram is illustrated in Fig. 8.

B. QFT Image Watermarking

The SCDFT scheme is attractive because it utilizes chromatic information to improve the imperceptibility of the watermarked image, but it ignores the luminance component. Attacks, such as JPEG compression and color to grayscale conversion, would destroy the watermark. To combat such attacks, a new color watermarking algorithm using the quaternion Fourier transform (QFT) is introduced [33].

1) *Quaternion Image Processing (QIP):* Quaternion image processing (QIP), proposed by Sangwine and Ell [34], is a new framework to exploit further information inherited among the channels of color images. Extensive research on QIP began in 1996, and the objective is to generalize different techniques from signal and image processing, such as frequency-domain filtering, correlation, and compression, to handle color images as vector images [35]. Compared to the SCIP, which can only handle data with two components, QIP can process data with up to four components. Since most color images only have three components (RGB, Lab, etc.), QIP is sufficient to process them as vectors, rather than separate scalars.

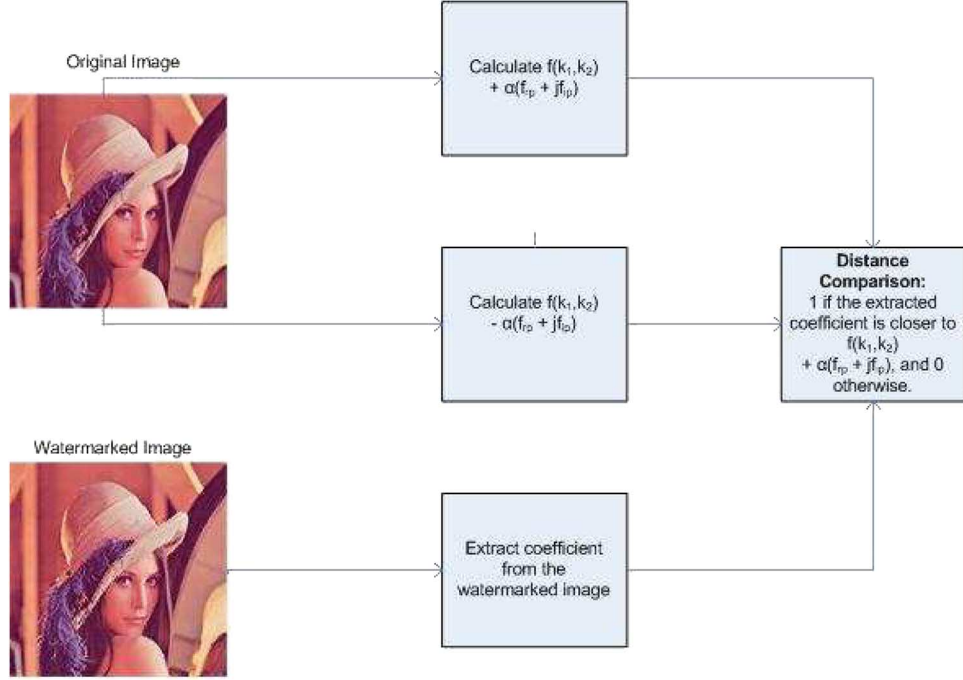


Fig. 8. Flow diagram showing the extraction procedure using the SCDFT scheme.

A quaternion number has one real and three orthogonal imaginary components. It is usually expressed in the form

$$Q = a + ib + jc + kd \quad (22)$$

where a , b , c , and d are scalar coefficients, and i , j , and k are imaginary operators that have the following characteristics:

$$\begin{aligned} i^2 = j^2 = k^2 = ijk = -1; \\ ij = k, jk = i, ki = j; \\ ji = -k, kj = -i, ik = -j. \end{aligned}$$

Given a quaternion Q , its conjugate is $Q^* = a - ib - jc - kd$ and its magnitude is $\sqrt{a^2 + b^2 + c^2 + d^2}$. It is sometimes useful to express Q into two parts: vector and scalar

$$Q = S(Q) + \mathbf{V}(Q) \quad (23)$$

where $S(Q) = a$ and $V(Q) = ib + jc + kd$. Note that multiplication of quaternions is not commutative, that is, $Q1 \times Q2 \neq Q2 \times Q1$.

Parallel and perpendicular decomposition: Given a pure quaternion u and a second pure unit quaternion v , u may be decomposed into components that are parallel and perpendicular to v as follows:

$$u_{\perp} = \frac{1}{2}(u + vuv) \quad (24)$$

where u_{\perp} is perpendicular to v , and

$$u_{\parallel} = \frac{1}{2}(u - vuv) \quad (25)$$

where u_{\parallel} is parallel to v .

Quaternion Fourier transform: The discrete QFT was first presented by Sangwine and Ell [36]. It is defined as

$$F(u, v) = \frac{1}{MN} \sum_{m=0}^{M-1} \sum_{n=0}^{N-1} e^{-i2\pi(\frac{mu}{M})} F(m, n) e^{-j2\pi(\frac{nv}{N})} \quad (26)$$

and the inverse QFT is formulated as

$$F(m, n) = \frac{1}{MN} \sum_{u=0}^{M-1} \sum_{v=0}^{N-1} e^{i2\pi(\frac{mu}{M})} F(u, v) e^{j2\pi(\frac{nv}{N})} \quad (27)$$

where M and N are the dimensions of the image.

To perform watermarking in the QFT domain, an interpretation to the QFT spectral points must be known. McCabe [24] provided an interpretation of the SCDFT coefficients, but a similar interpretation to the QFT coefficients is not available. The first question that comes to mind is: How does embedding watermarks in the QFT coefficients affect the image $F(m, n)$ in the spatial domain? Before answering this question, a general framework is needed to interpret the quaternion spectral points of color images. To achieve this goal, McCabe's interpretation will be extended to the QFT domain.

2) *Spectrum Interpretation:* Having introduced the concept of phasors in the SCIP, let us expand (27). Let $\theta_1 = 2\pi(mu/M)$, $\theta_2 = 2\pi(nv/N)$, $F(u, v) = a_1 + b_1i + c_1j + d_1k$ and $F(-u, -v) = a_2 + b_2i + c_2j + d_2k$. This then gives

$$\begin{aligned} e^{i\theta_1} F(u, v) e^{j\theta_2} \\ = a_1 \cos \theta_1 \cos \theta_2 - c_1 \cos \theta_1 \sin \theta_2 - b_1 \sin \theta_1 \cos \theta_2 \\ + d_1 \sin \theta_1 \sin \theta_2 + i(b_1 \cos \theta_1 \cos \theta_2 - d_1 \cos \theta_1 \sin \theta_2 \\ + a_1 \sin \theta_1 \cos \theta_2 - c_1 \sin \theta_1 \sin \theta_2) \\ + j(a_1 \cos \theta_1 \sin \theta_2 + c_1 \cos \theta_1 \cos \theta_2 - b_1 \sin \theta_1 \sin \theta_2) \end{aligned}$$

$$\begin{aligned}
& -d_1 \sin \theta_1 \cos \theta_2) \\
& + k(b_1 \cos \theta_1 \sin \theta_2 + d_1 \cos \theta_1 \cos \theta_2 + a_1 \sin \theta_1 \sin \theta_2 \\
& \quad + c_1 \sin \theta_1 \cos \theta_2), \quad (28) \\
& e^{-i\theta_1} F(-u, -v) e^{-j\theta_2} \\
& = a_2 \cos \theta_1 \cos \theta_2 + c_2 \cos \theta_1 \sin \theta_2 + b_2 \sin \theta_1 \cos \theta_2 \\
& \quad + d_2 \sin \theta_1 \sin \theta_2 + i(b_2 \cos \theta_1 \cos \theta_2 + d_2 \cos \theta_1 \sin \theta_2 \\
& \quad \quad - a_2 \sin \theta_1 \cos \theta_2 - c_2 \sin \theta_1 \sin \theta_2) \\
& \quad + j(-a_2 \cos \theta_1 \sin \theta_2 + c_2 \cos \theta_1 \cos \theta_2 - b_2 \sin \theta_1 \sin \theta_2 \\
& \quad \quad + d_2 \sin \theta_1 \cos \theta_2) \\
& \quad + k(-b_2 \cos \theta_1 \sin \theta_2 + d_2 \cos \theta_1 \cos \theta_2 \\
& \quad \quad + a_2 \sin \theta_1 \sin \theta_2 - c_2 \sin \theta_1 \cos \theta_2). \quad (29)
\end{aligned}$$

Considerable simplifications can be made to (28) and (29), and an interpretation of the QFT coefficients can be drawn if the parameters $a_1, a_2, b_1, b_2, \dots$ are assigned in certain ways. There are four cases of interest. Let $F(\pm u, \pm v)$ denote $F(u, v) = F(-u, -v)$.

Case 1) $F(\pm u, \pm v) = dk$, then the summation of (28) and (29) gives

$$2d \sin \theta_1 \sin \theta_2 + k2d \cos \theta_1 \cos \theta_2. \quad (30)$$

Equation (30) shows that if $F(\pm u, \pm v) = dk$, then the combined effect of the positive and negative coefficients is the same as a cosine function with a magnitude of $2d$ varying along the k component (the real component of the image is ignored).

Case 2) $F(\pm u, \pm v) = bi$, then the summation of (28) and (29) gives

$$i2b \cos \theta_1 \cos \theta_2 - j2b \sin \theta_1 \sin \theta_2. \quad (31)$$

Equation (31) shows that if $F(\pm u, \pm v) = bi$, then the combined effects of the positive and negative coefficients are the same as a circle with diameter $2b$, starting at angle 0, rotating in the negative direction on a complex plane.

Case 3) $F(\pm u, \pm v) = cj$, then the summation of (28) and (29) gives

$$-i2c \sin \theta_1 \sin \theta_2 + j2c \cos \theta_1 \cos \theta_2. \quad (32)$$

Equation (32) shows that if $F(\pm u, \pm v) = cj$, then the combined effects of the positive and negative coefficients are the same as a circle with diameter $2c$, starting at angle $\pi/2$, rotating in the negative direction on a complex plane.

Case 4) $F(\pm u, \pm v) = bi + cj + dk$ can be interpreted as the combinations of Cases 1), 2), and 3).

If we encode a color image as $F(m, n) = b^*(m, n)i + c^*(m, n)j + L^*(m, n)k$, using the interpretation from before, some conclusions can be made:

Case 1) $F(\pm u, \pm v) = dk$ can be interpreted as adding a cosine function in the luminance component of the image.

Cases 2 and 3) $F(\pm u, \pm v) = bi$ or $F(\pm u, \pm v) = cj$ enables us to use the interpretations provided by McCabe, as in



Fig. 9. Different watermark patterns. (a) $W(\pm u, \pm v) = L^*k$. (b) $W(\pm u, \pm v) = b^*i$. (c) $W(\pm u, \pm v) = c^*j$.

the SCDFD domain, to add a function, in the form of a rainbow grating in the chromatic components of the image. The watermark patterns of Cases 1), 2), and 3) are shown in Fig. 9.

Case 4) $F(\pm u, \pm v) = bi + cj + dk$ can be interpreted as a cosine grating embedded in the luminance component and two rainbow gratings rotating with the same direction and different initial angles in the chrominance components.

3) *New Adaptive Color Watermarking Algorithm*: The interpretation of the QFT coefficients is very important to predict the possible change made to the image after watermarking. In the context of digital image watermarking, the goal is to design a watermark $W(u, v)$, with the scaling factor α as big as possible, such that the visible distortion to the image is perceptually minimal. Mathematically speaking, the watermarked image $WF(m, n)$ can be formulated as

$$\begin{aligned}
WF(m, n) &= IQFT(F(u, v) + \alpha W(u, v)) \\
&= IQFT(F(u, v)) + IQFT(\alpha W(u, v)) \\
&= F(m, n) + W(m, n). \quad (33)
\end{aligned}$$

Let $W(\pm u, \pm v) = b_3i + c_3j + d_3k$. b_3, c_3 , and d_3 can be designed according to the guidelines given in the previous section. The component b_3 would add the watermark in the luminance component, where c_3 and d_3 are responsible for the chromatic components. In order to make the overall effect vary along the yellow–blue axis, as we did in the SCDFD scheme, some constraints must be imposed to the values b_3, c_3 , and d_3 . From (31) and (32), if $b_3 = c_3$, the summation of (31) and (32) becomes

$$i2b_3(\cos \theta_1 \cos \theta_2 - \sin \theta_1 \sin \theta_2) + j2b_3(\cos \theta_1 \cos \theta_2 - \sin \theta_1 \sin \theta_2) = 2b_3(\cos \theta_1 \cos \theta_2 - \sin \theta_1 \sin \theta_2)(i + j) \quad (34)$$

and the overall effect would vary along the 45° axis. It means the color of the overall effect would be red and blue. To satisfy the requirement of varying along the yellow–blue axis, we have to transform the a^*b^* by 45° before taking the QFT of the image $F(m, n)$ such that it would align with the $+b$ and $-b$ axis and oscillate between yellow and blue.

Since the sensitivity of the HVS to the yellow–blue component is approximately $1/5$ compared to the luminance component [7], we can set $d_3 = (1/5)b_3$, which gives

$$W(\pm u, \pm v) = b_3i + b_3j + \frac{1}{5}b_3k. \quad (35)$$

To ensure invisibility of the watermark, a distortion metric $D(n, m, u, v)$ is defined to measure the difference in the spatial

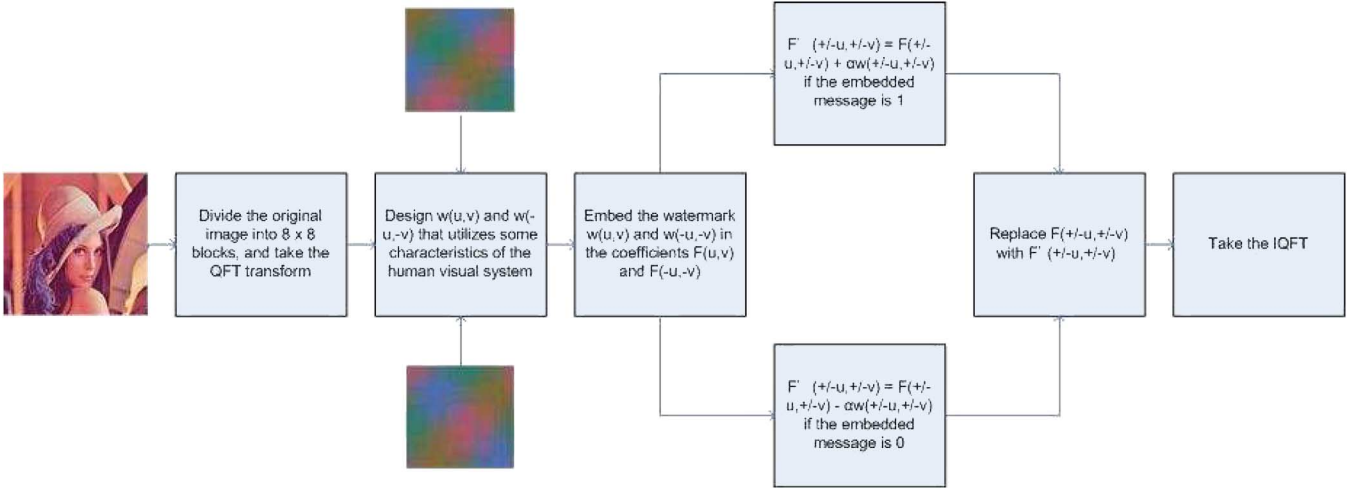


Fig. 10. Flow diagram showing the insertion procedure using the QFT scheme.

domain generated by adding the coefficients $W(u, v)$ and $W(-u, -v)$ in the frequency domain, defined as

$$D(n, m, u, v) = \frac{\alpha}{N^2} \left(i2b_3(\cos \theta_1 \cos \theta_2 - \sin \theta_1 \sin \theta_2) + j2b_3 \cos \theta_1 \cos \theta_2 - \sin \theta_1 \sin \theta_2 + k\frac{2}{5}b_3 \cos \theta_1 \cos \theta_2 \right) \leq \text{NUJNCD}. \quad (36)$$

Again, watermark invisibility is achieved if the distortion of the watermarked image is smaller than the quantity NUJNCD, $\|D(n, m, u, v)\|^2 \leq (\text{NUJNCD})^2 \forall n, m$, that is

$$\|D(n, m, u, v)\|^2 = \frac{\alpha^2}{N^4} \left(8(b_3(\cos \theta_1 \cos \theta_2 - \sin \theta_1 \sin \theta_2))^2 \times \frac{4}{25}(b_3 \cos \theta_1 \cos \theta_2)^2 \right) \leq (\text{NUJNCD})^2. \quad (37)$$

The parameter α is an important factor, because the larger it is, the more robust the watermarked image will be. Depending on the perceptual requirement of the applications, two options are available to maximize α . One is to make the average distortions of a block less than NUJNCD (loose condition), and the other one is to make the distortion of every pixel less than NUJNCD (tight condition).

Approach 1: Calculate α such that the average distortion of a block is less than NUJNCD

$$\begin{aligned} \|D(u, v)\|^2 &= \frac{\alpha^2}{N^4} \sum_{n=0}^{N-1} \sum_{m=0}^{N-1} 8(b_3(\cos \theta_1 \cos \theta_2 - \sin \theta_1 \sin \theta_2))^2 \\ &\quad \times \frac{4}{25}(b_3 \cos \theta_1 \cos \theta_2)^2 \\ &= N^2(\text{NUJNCD})^2. \end{aligned} \quad (38)$$

Let $x = \cos \theta_1 \cos \theta_2 - \sin \theta_1 \sin \theta_2$ and $y = \cos \theta_1 \cos \theta_2$

$$\alpha = \sqrt{\frac{N^6(\text{NUJNCD})^2}{\sum_{n=0}^{N-1} \sum_{m=0}^{N-1} 8(b_3x)^2 + \frac{4}{25}(b_3y)^2}}. \quad (39)$$

Approach 2: Recursively decrease α until the distortions of all pixels are smaller than NUJNCD. An initial α is assigned, and calculate $\|D(n, m, u, v)\|^2$ for every pixel of the block. If some pixel distortion exceeds $(\text{NUJNCD})^2$, we decrease α until $\|D(n, m, u, v)\|^2 < (\text{NUJNCD})^2 \forall n, m$.

4) Embedding and Decoding Procedures: Given an image of size $N \times N$, the image is divided into blocks of size 8×8 , followed by taking the QFT of each block. We embed a pair of marks $W(u', v')$ and $W(-u', -v')$ into the coefficients $F(u', v')$ and $F(-u', -v')$ in the following way:

$$WF(u', v') = F(u', v') \pm \alpha W(u', v') \quad (40)$$

$$WF(-u', -v') = F(-u', -v') \pm \alpha W(-u', -v') \quad (41)$$

where α is the watermark strength to be maximized. Set $W(u', v') = (0, b_3, b_3, (1/5)b_3)$ and $W(-u', -v') = (0, b_3, b_3, (1/5)b_3)$ to generate watermarks that vary along the luminance and yellow-blue component. Notice that the real component is ignored when converting the watermarked image back to the La^*b^* color space; therefore, the real component $Re(m, n)$ is kept, as a key when extracting the watermark. The flow diagram showing the insertion procedure in the QFT domain is shown in Fig. 10.

To decode the embedded watermark $W(u, v)$, the original image $F(m, n)$, the watermarked (possibly corrupted) image $WF(m, n)$, and $Re(m, n)$ are needed. First, the image is encoded to quaternion format, and then replace the real component of $WF(m, n)$ with $Re(m, n)$, followed by taking the QFT of both images. Then, $F(u', v') + \alpha W(u', v')$ and $F(u', v') - \alpha W(u', v')$ are calculated from the original image, followed by a distance comparison to the coefficient extracted from $WF(u', v')$. If the extracted coefficient is closer to

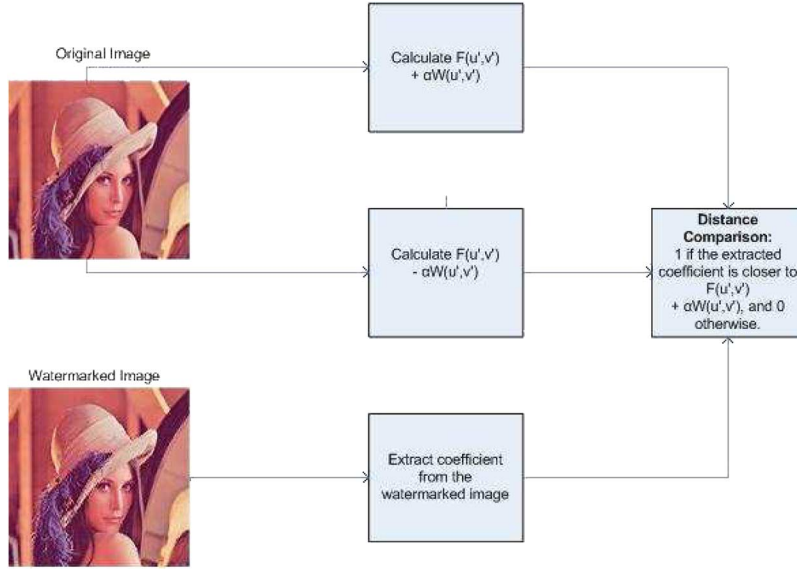


Fig. 11. Flow diagram showing the extraction procedure using the QFT scheme.

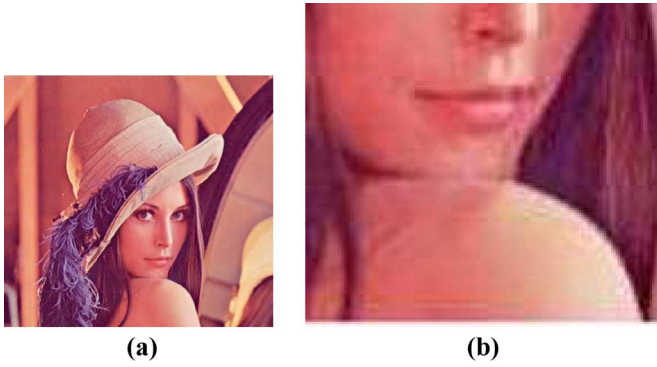


Fig. 12. (a) Original Lenna image. (b) Magnified version of the top left corner of (a).



Fig. 13. (a) Watermarked Lenna image using the SCDFT. (b) Magnified version of the top left corner of (a).

$F(u', v') + \alpha W(u', v')$, bit 1 was embedded; otherwise, bit 0 was embedded. The flow diagram is shown in Fig. 11.

IV. SIMULATION RESULTS

In order to prove that the algorithms and theories described before indeed increase the robustness of the watermarked images against attacks, a series of experiments has been conducted by applying the attacks to the Lenna image of size 512×480 . The attacks include:

- image compression—JPEG;
- geometric transformations—resizing, rotation, shearing, cropping;
- image enhancement—sharpening, and histogram equalization;
- color manipulation—color to grayscale conversion;
- information reduction—Gaussian noise.

One bit of information was embedded into each block imperceptibly using the aforementioned watermarking techniques on $AC(2, 2)$ and $AC(6, 6)$, where (2,2) and (6,6) indicate the coordinates of the spatial frequency. The original Lenna images are shown in Fig. 12(a), and 3840 b of information were embedded into each image. Fig. 13(a) shows the watermarked images using



Fig. 14. (a) Watermarked Lenna image using the QFT. (b) Magnified version of the top left corner of (a).

the SCDFT approach, where the watermarked images using the QFT approach are shown in Fig. 14(a).

In order to test the robustness of the algorithms, some common attacks were applied, and the results were compared to two well-known watermarking algorithms—the DCT based and ac estimation-based methods [14]. The peak signal-to-noise ratios (PSNRs) and the number of bits embedded in the Lenna image using the SCDFT, QFT, DCT, and ac algorithms are: (30.1027, 3840 b), (30.9283, 3840 b), (30.4064, 3840 b), and



Fig. 15. (a) Watermarked Lenna image using ac estimation. (b) Magnified version of the top left corner of (a).



Fig. 16. (a) Watermarked Lenna image using the DCT. (b) Magnified version of the top left corner of (a).

TABLE I
LENNA IMAGE: BERs AGAINST THE ATTACKS

| Attack | SCDFT | QFT | DCT | AC |
|------------------------|--------|--------|-------|-------|
| No attack | 0% | 0% | 0% | 0% |
| Histogram Equalization | 0% | 0% | 3% | 0% |
| Sharpening | 0% | 0% | 4% | 0.24% |
| Blurring | 0% | 0% | 3% | 0% |
| Resizing by factor 2 | 6.58% | 0% | 4.87% | 0% |
| Rotation | N/A | N/A | N/A | N/A |
| Shearing | N/A | N/A | N/A | N/A |
| Cropping | N/A | N/A | N/A | N/A |
| Color to greyscale | 49.96% | 30.14% | 0% | 0% |

(30.1081, 416 b), respectively. Notice that the PSNRs are adjusted to be about the same in order to reflect the power of the embedded watermarks to also be the same. The distortions generated by the ac and DCT algorithms in Figs. 15 and 16, respectively, are much more visible. The underlying reason is because these methods only embed watermarks in the luminance component, which ignores the masking effects of the chrominance components. Table I shows the bit-error rates (BERs) against histogram equalization, sharpening, blurring, resizing, and color to grayscale conversion. The results for the robustness against JPEG compression and Gaussian noise are shown in Figs. 17 and 18.

From the measurements, several observations can be made.

- SCDFT approach: This scheme provides satisfactory results for most attacks. In addition, the compensation mark does reduce the visible distortion. Notice that the watermarked images using other schemes have perceptual artifacts under the same PSNR, where the SCDFT scheme does not. However, it is Not robust against JPEG compression, especially when the compression factor is low

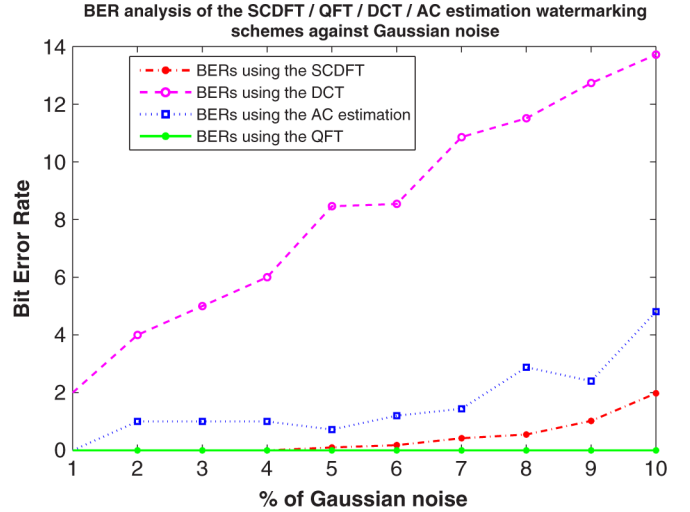


Fig. 17. Lenna image: BERs against Gaussian noise.

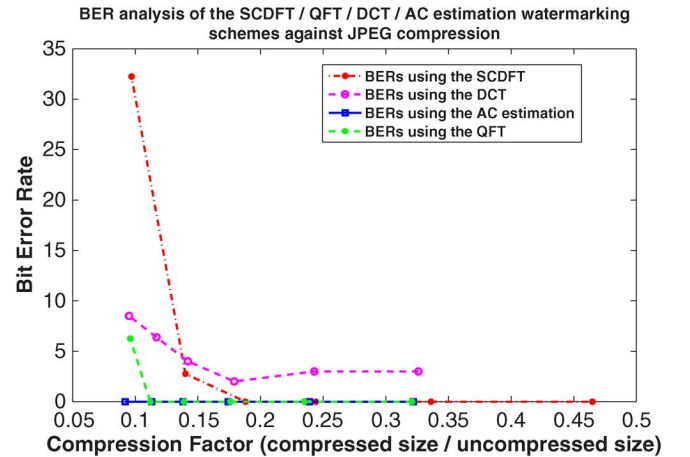


Fig. 18. Lenna image: BERs against JPEG compression.

(compression factor = compressed size/uncompressed size). The underlying reason is that the SCDFT algorithm only modifies the chromatic components of a color image, and JPEG quantizes them aggressively for high compression, which corrupts the watermark as the compression factor goes down. In addition, the watermark is completely destroyed if the image is converted to grayscale. The underlying reason is because the watermark resides in the chromatic components.

- QFT approach: The most successful scheme effectively solves the problem that the SCDFT has. The underlying reason is that the watermark is spread evenly among the luminance and chrominance components of the images. Also, the compensation mark allows the watermark to be undetected even if the strength of it is high. Even though it cannot completely recover the embedded messages for a low compression factor, the BER is significantly smaller than the SCDFT approach. Compared to the SCDFT approach, this scheme significantly reduces the BER rate for converting color to grayscale images by approximately 30%, because the watermark is embedded in the luminance as well as chrominance components. One small disadvantage of it is that the computational complexity is high for quaternion algebras.

- AC estimation method: It provides very good results for most attacks, and the biggest advantage of it is that it is a blind watermarking scheme. However, it has two major drawbacks—due to the nature of the algorithm, not every coefficient is suitable for modification. As a result, the maximum number of bits that can be embedded is much smaller, and the visible distortion is detectable at the same PSNR.
- DCT approach: Even though it still provides satisfactory results, the BERs of the attacks are generally higher. The underlying reason is that most existing DCT-based algorithms do not embed watermarks in every single block of a image. They selectively pick the regions that do not generate visible distortion (for example, highly textured regions) for embedding, thus decreasing the data payload, but increasing the accuracy of extraction. In the experiments performed in this paper, in order to show that the proposed algorithms (i.e., SCDF and QFT) can accept watermark in all regions (due to the compensation mark), this constraint was removed, and the watermarks were embedded in every block of the image. In addition, since this algorithm only embeds the watermark in the luminance component, ignoring the masking effects of the chromatic components, the imperceptibility of it is not as good. However, it only requires limited computational power due to the high availability of fast algorithms to compute the DCT and DFT.

Another observation is that the proposed approach does not perfectly resist the color-grayscale conversion. The underlying reason is because a portion of the watermarks is embedded in the chromatic content of the images. As a result, if these contents are removed, some errors would occur, which would relate to visual distortion in the image, thus signalling a tampering of the image, which is a fundamental requirement of all nonblind techniques. Furthermore, the fact that a portion of the watermark is present in the chrominance and the luminance provides robustness to an attack, which aims to remove the luminance component since some portions of the watermark reside in the chrominance components. In other words, the proposed algorithm uses a balanced approach that evenly and robustly distributes the watermark into all components.

Even though the scheme is a nonblind watermarking scheme, it still has lots of applications, such as transaction tracking and copy control. Under these circumstances, we assume that the original image is available; therefore, the developed algorithms are not designed for attacks that would seriously distort the watermarked image. Notice that all algorithms are not robust to desynchronization attacks, such as shearing and cropping. The underlying reason is that our algorithms are nonblind algorithms, which require the original image for watermark extraction. If the coordinates of the pixels of the watermarked images are shifted, the watermarks could not be extracted unless the coordinates of the pixels of the original image are shifted by the same amount. Nevertheless, desynchronization attacks would make the distortion on the watermarked images so visible. As a result, given the original image, we would immediately know the watermarked images have been attacked. Thus, it is not necessary for our algorithms to withstand desynchronization attacks.

V. CONCLUSION

Color is a very important content in images. Most existing watermarking schemes only utilize the luminance content for watermarking. At the time of the publication of this paper, there is only one comparable algorithm that also uses the QFT for watermarking [23]. However, that algorithm uses the empirical method to calculate the strength of the watermark that is suitable for the testing image they used, which does not work for all images. Our algorithms use the adaptive approach to obtain the optimal strength of the watermark based on the local characteristics of different images.

We investigated a new approach for embedding watermarks into all components (luminance and chrominance) of color images. The idea is inspired by the fact that colors can be added and subtracted to produce other colors. The technique explores the interpretation of the complex components of the frequency components using the two transforms, and utilizes the characteristic that human eyes are insensitive to yellow and blue to develop two embedding algorithms. By embedding two marks (i.e., watermark and compensation mark) in the coefficients, a composite mark that only contains insensitive colors is able to produce. Results demonstrate the proposed algorithms are robust to many digital signal processing operations and external attacks, because the strength of the watermark is maximized, whereas the imperceptibility is also maximized due to the reason that the compensation mark reduces the perceptual distortion generated by adding the watermark.

Future work can be extended as follows.

- Cross-masking effects between the luminance and chrominance components—the interaction between the luminance and chrominance components can be further analyzed [37] in order to improve the imperceptibility of the watermarked images.
- The proposed algorithms can be extended such that watermarks can be embedded into multiple frequency coefficients.
- Greater understanding of the QFT spectral coefficients is helpful to provide a more sophisticated watermarking algorithm.
- A better estimation of the upper bound JNCD can be calculated by incorporating more characteristics of the HVS.
- The theories might be applicable to other similar fields, such as color image coding and color image compression.

Watermarking algorithms considering both luminance and chromatic components of color images in a holistic manner are expected to be the future trend of development.

REFERENCES

- [1] K. Tanaka, Y. Nakamura, and K. Matsui, "Embedding secret information into a dithered multi-level image," in *Proc. IEEE MILCOM Int. Conf.*, 1990, pp. 216–220.
- [2] I.-K. Yeo and H. J. Kim, "Modified patchwork algorithm: A novel audio watermarking scheme," in *Proc. Int. Conf. Information Technology: Coding Computing*, 2001, p. 237.
- [3] N. Cvejic and I. Tujkovic, "Increasing robustness of patchwork audio watermarking algorithm using attack characterization," in *Proc. IEEE Int. Symp. Consumer Electronics*, U.K., 2004, pp. 3–6.
- [4] N. Cvejic and T. Seppanen, "Robust audio watermarking in wavelet domain using frequency hopping and patchwork method," in *Proc. 3rd Int. Symp. Image Signal Processing Analysis*, Rome, Italy, 2003, pp. 251–255.

- [5] A. Z. Tirkel, G. A. Rankin, R. G. van Schyndel, W. J. Ho, N. R. A. Mee, and C. F. Osborne, *Electronic Watermark*. In *Digital Image Computing, Technology and Applications*. Sydney, Australia, Dec. 1993, pp. 666–672.
- [6] B. Chen and G. Wornell, “Quantization index modulation methods for digital watermarking and information embedding of multimedia,” *J. VLSI Signal Process.*, p. 7V33, 2001.
- [7] B. A. Wandell, *Foundations of Vision*. Sunderland, MA: Sinauer Associates, 1995.
- [8] I. Cox, J. Killian, T. Leighton, and T. Shamoan, “Secure spread spectrum watermarking for images, audio and video,” in *Proc. IEEE Int. Conf. Image Processing*, Lausanne, Switzerland, Sep. 16–19, 1996, vol. 111, pp. 243–246.
- [9] I. J. Cox, J. Killian, F. T. Leighton, and T. Shamoan, “Secure spread spectrum watermarking for multimedia,” *IEEE Trans. Image Process.*, vol. 6, no. 12, pp. 1673–1687, Dec. 1997.
- [10] A. Piva, F. Bartolinin, V. Cappellini, and M. Barni, “Exploiting the cross-correlation of rgb-channels for robust watermarking of color images,” in *Proc. Int. Conf. Image Processing*, Kobe, Japan, Oct. 24–28, 1999, vol. 1, pp. 306–310.
- [11] N. Ahmadi and R. Safabakhsh, “A novel dct-based approach for secure color image watermarking,” in *Proc. Int. Conf. Information Technology: Coding and Computing*, Apr. 2004, vol. 2, pp. 709–713.
- [12] C.-H. Chou and Y.-C. Li, “A perceptually tuned subband image coder based on the measure of just-noticeable distortion profile,” *IEEE Trans. Circuits Syst. Video Technol.*, vol. 5, no. 6, pp. 467–476, Dec. 1995.
- [13] L. Ghouti and A. Bouridane, “A just-noticeable distortion (jnd) profile for balanced multiwavelets,” presented at the Eur. Signal Processing Conf., 2005.
- [14] Y. Wang and A. Pearmain, “Ac estimation-based image watermarking method,” presented at the 5th Eur. Workshop Image Analysis Multimedia, Lisbon, Portugal, Apr. 2004.
- [15] C. Podilchuk and W. Zeng, “Image-adaptive watermarking using visual models,” *IEEE J. Sel. Areas Commun.*, vol. 16, no. 4, pp. 525–539, May 1998.
- [16] K. R. N. Kaewkamnerd, “Wavelet based image adaptive watermarking scheme,” *Electron. Lett.*, vol. 36, pp. 518–526, 2000.
- [17] A. Piva, L. Boccardi, F. B. M. Barni, V. Cappellini, and A. D. Rosa, “Watermarking through color image bands decorrelation,” in *Proc. IEEE Int. Conf. Multimedia Expo.*, New York, Jul. 30–Aug. 2, 2000, pp. 1283–1286.
- [18] S. Gilani and A. Skodras, “Dlt-based digital image watermarking,” presented at the 1st IEEE Balkan Conf. Communications, Circuits Systems, Istanbul, Turkey, Jun. 2–3, 2000.
- [19] A. Ho, J. Shen, and S. Tan, “Robust digital image-in-image watermarking algorithm using the fast hadamard transform,” presented at the SPIE 4793, 2002.
- [20] S. A. M. Gilani, I. Kostopoulos, and A. N. Skodras, “Color image-adaptive watermarking,” in *Proc. 14th Int. Conf. Digital Signal Processing*, Santorini, Greece, Jul. 1–3, 2002, pp. 721–724.
- [21] V. Licks and R. Jordan, “On digital image watermarking robust to geometric transformations,” 2000. [Online]. Available: citeseer.ist.psu.edu/article/licks00digital.html.
- [22] A. Reed and B. Hannigan, “Adaptive color watermarking,” in *Proc. SPIE 4675*, Apr. 2002, p. 222.
- [23] P. Bas, N. L. Bihan, and J. Chassery, “Color watermarking using quaternion Fourier transform,” in *Proc. ICASSP*, Hong Kong, China, Jun. 2003, pp. 521–524.
- [24] A. McCabe and T. Caelli, “Theory of spatiochromatic image encoding and feature extraction,” *J. Opt. Soc. Amer. A*, pp. 1744–1754, Oct 2000.
- [25] Y. Shi and H. Sun, *Image and Video Compression for Multimedia Engineering: Fundamentals, Algorithms and Standards*. Boca Raton, FL: CRC, 1999.
- [26] B. Watson, “Dct quantization matrices visually optimized for individual images,” in *SPIE: Human Vis., Vis. Process. Digital Display IV*, 1993, vol. 1913, pp. 202–216.
- [27] J. J. N. Jayant and R. Safranek, “Signal compression based on model of human perception,” *Proc. IEEE*, vol. 81, no. 10, pp. 1385–1421, Oct 1993.
- [28] M. D. Swanson, M. Kobayashi, and A. H. Tewfik, “Multimedia data embedding and watermarking technologies,” *Proc. IEEE*, vol. 86, no. 6, pp. 1064–1087, Jun. 1998.
- [29] B. Watson, “Efficiency of a model human image code,” *J. Opt. Soc. Am.*, vol. 4, p. 2401V2416, Dec. 1987.
- [30] C.-H. Chou and K.-C. Liu, “An oblivious and robust watermarking scheme using perceptual model,” in *Proc. Conf. Video Processing Multimedia Communications*, 2003, pp. 713–720.
- [31] R. G. Kuehni, *Color Space and Its Divisions: Color Order From Antiquity to the Present*. New York: Wiley, Feb. 2003.
- [32] T. Tsui, X. Zhang, and D. Androustos, “Color image watermarking using the spatio-chromatic fourier transform,” in *Proc. ICASSP*, Toulouse, France, May 2006, pp. 305–308.
- [33] T. Tsui, X. Zhang, and D. Androustos, “Quaternion image watermarking using the spatio-chromatic fourier coefficients analysis,” presented at the ACM, Santa Barbara, CA, Oct 2006.
- [34] S. J. Sangwine, “The problem of defining the fourier transform of a colour image,” in *Proc. ICIP*, Chicago, IL, Oct. 4–7, 1998, pp. 171–175.
- [35] S. J. Sangwine, “Colour image edge detector based on quaternion convolution,” *Electron. Lett.*, pp. 969–971, May 1998.
- [36] S. J. Sangwine and T. A. Ell, “The discrete fourier transforms of a colour image,” *Image Processing Mathematical Methods, Algorithms and Applications*, vol. 2000, pp. 430–441.
- [37] Y. Meng and L. Guo, “Color image coding by utilizing the crossed masking,” in *Proc. ICASSP*, vol. 2005, pp. 389–392.

Tsz Kin Tsui received the B.A.Sc. degree in electrical and computer engineering from the University of Toronto, Toronto, ON, Canada, in 2004 and the M.A.Sc. degree in electrical and computer engineering from Ryerson University, Toronto, ON, Canada, in 2006.

Currently, he is with Research In Motion, Waterloo, ON, Canada. His research interests are in image watermarking, multimedia data hiding, and image segmentation.

Xiao-Ping Zhang (SM’02) received the B.S. and Ph.D. degrees in electronic engineering from Tsinghua University, Beijing, China, in 1992 and 1996, respectively.

Currently, he is an Associate Professor and Director of Communication and Signal Processing Applications Laboratory (CASPAL) with the Department of Electrical and Computer Engineering, Ryerson University, Toronto, ON, Canada. Prior to joining Ryerson, from 1996 to 1998, he was a Postdoctoral Fellow at the University of Texas, San Antonio, and then at the Beckman Institute, the University of Illinois at Urbana-Champaign. He held research and teaching positions at the Communication Research Laboratory with McMaster University, Hamilton, ON, Canada, in 1999. From 1999 to 2000, he was a Senior DSP Engineer with SAM Technology, Inc., San Francisco, CA, and a Consultant with the San Francisco Brain Research Institute, San Francisco. His research interests include signal processing for communications, multimedia data hiding, retrieval and analysis, computational intelligence, and applications in bioinformatics and finance. He is a frequent Consultant for biotech companies and was the Publicity Co-Chair for ICME’06 and Program Co-Chair for ICIC’05.

Dr. Zhang received the Science and Technology Progress Award from the State Education Commission of China, for his significant contribution to a National High-Tech Project, in 1994. He is a registered Professional Engineer in Ontario, Canada.

Dimitrios Androustos (SM’05) received the B.A.Sc., M.A.Sc., and Ph.D. degrees in electrical engineering from the University of Toronto, Toronto, ON, Canada, in 1992, 1994, and 1999, respectively.

Currently, he is an Associate Professor and Program Director for Electrical Engineering in the Department of Electrical and Computer Engineering with Ryerson University, Toronto. Prior to joining Ryerson University, he was a Software Engineer in the area of digital cinema with A.F. Associates, Northvale, NJ. He was an Imaging Scientist with Finline Technologies, Waterloo, ON, Canada, working in the area of image and video compression using wavelets and, subsequently, he was a Senior DSP Engineer in the Advanced Technology Group of SOMA Networks, Toronto. His research interests are in image, video, and multimedia processing and retrieval, digital cinema, 3-D imaging and video, and computational image processing.

Dr. Androustos has been a Guest Editor for *IEEE Signal Processing Magazine*, the Exhibit Chair of ICME’06, the General Chair of ICUE’07, and is currently the Plenary Chair for CCECE’08 and the Membership Development Chair of the Toronto Section of the IEEE. He is a registered Professional Engineer (P.Eng) in Ontario, Canada, and a Sigma Xi member.